

# Effective Connectivity in Autism

Edmund T. Rolls , Yunyi Zhou, Wei Cheng, Matthieu Gilson, Gustavo Deco, and Jianfeng Feng

The aim was to go beyond functional connectivity, by measuring in the first large-scale study differences in effective, that is directed, connectivity between brain areas in autism compared to controls. Resting-state functional magnetic resonance imaging was analyzed from the Autism Brain Imaging Data Exchange (ABIDE) data set in 394 people with autism spectrum disorder and 473 controls, and effective connectivity (EC) was measured between 94 brain areas. First, in autism, the middle temporal gyrus and other temporal areas had lower effective connectivities to the precuneus and cuneus, and these were correlated with the Autism Diagnostic Observational Schedule total, communication, and social scores. This lower EC from areas implicated in face expression analysis and theory of mind to the precuneus and cuneus implicated in the sense of self may relate to the poor understanding of the implications of face expression inputs for oneself in autism, and to the reduced theory of mind. Second, the hippocampus and amygdala had higher EC to the middle temporal gyrus in autism, and these are thought to be back projections based on anatomical evidence and are weaker than in the other direction. This may be related to increased retrieval of recent and emotional memories in autism. Third, some prefrontal cortex areas had higher EC with each other and with the precuneus and cuneus. Fourth, there was decreased EC from the temporal pole to the ventromedial prefrontal cortex, and there was evidence for lower activity in the ventromedial prefrontal cortex, a brain area implicated in emotion-related decision-making. *Autism Res* 2020, 13: 32–44. © 2019 International Society for Autism Research, Wiley Periodicals, Inc.

**Lay Summary:** To understand autism spectrum disorders better, it may be helpful to understand whether brain systems cause effects on each other differently in people with autism. In this first large-scale neuroimaging investigation of effective connectivity in people with autism, it is shown that parts of the temporal lobe involved in facial expression identification and theory of mind have weaker effects on the precuneus and cuneus implicated in the sense of self. This may relate to the poor understanding of the implications of face expression inputs for oneself in autism, and to the reduced theory of mind.

**Keywords:** autism; effective connectivity; face expression; temporal cortex; precuneus; amygdala

## Introduction

Autism spectrum disorder (ASD) is a complex developmental disorder that is characterized by difficulties in social communication and social interaction; and restricted and repetitive behavior, interests, or activities [Lai, Lombardo, & Baron-Cohen, 2014]. Recently, a great deal of attention has been focused on the delineation of neural systems for brain–behavior relationships in ASD given that ~1% of children are being diagnosed with this disorder [Kim et al., 2011]. At the brain circuit level, resting-state functional magnetic resonance imaging (fMRI) studies are contributing to our understanding of brain systems related to autism [Hull et al., 2016; Maximo, Cadena, & Kana, 2014]. These studies have suggested abnormality in connectivity between a group

of related and partly overlapping brain systems characterized as face processing areas [Cheng, Rolls, Gu, Zhang, & Feng, 2015; Koshino et al., 2008], the default mode network [Padmanabhan, Lynch, Schaer, & Menon, 2017], social brain circuits [Gotts et al., 2012], theory of mind areas [Cheng et al., 2015], self-representation circuitry [Cheng et al., 2015; Lombardo et al., 2010], reward circuitry [Dichter et al., 2012], the salience network [Uddin et al., 2013], and a motor control network [Kenet et al., 2012]. In a recent large-scale study (418 people with autism and 509 controls), a key system in the middle temporal gyrus/superior temporal sulcus region, which is implicated in the face expression processing and theory of mind involved in social behavior had reduced functional connectivity with the ventromedial prefrontal cortex (VMPFC), which is implicated in emotion and social

From the Department of Computer Science, University of Warwick, Coventry, UK (E.T.R., J.F.); Oxford Centre for Computational Neuroscience, Oxford, UK (E.T.R.); Institute of Science and Technology for Brain-inspired Intelligence, Fudan University, Shanghai, China (E.T.R., Y.Z., W.C., J.F.); Center for Brain and Cognition, Computational Neuroscience Group, Department of Information and Communication Technologies, Universitat Pompeu Fabra, Barcelona, Spain (M.G., G.D.); Institució Catalana de la Recerca i Estudis Avançats (ICREA), Universitat Pompeu Fabra, Barcelona, Spain (G.D.)

Edmund T. Rolls, Yunyi Zhou, and Wei Cheng are co-first authors.

Received June 5, 2019; accepted for publication October 3, 2019

Address for correspondence and reprints: Edmund T. Rolls, Department of Computer Science, University of Warwick, Coventry CV4 7AL, UK. E-mail: edmund.rolls@oxcns.org

Published online 27 October 2019 in Wiley Online Library (wileyonlinelibrary.com)

DOI: 10.1002/aur.2235

© 2019 International Society for Autism Research, Wiley Periodicals, Inc.

communication [Cheng et al., 2015]. A second key system in the precuneus/superior parietal lobule region, which is implicated in spatial functions including of oneself, and of the spatial environment, also had reduced functional connectivity in autism [Cheng et al., 2015].

Resting-state functional connectivity, which reflects correlations in the activity between brain areas, is widely used to help understand human brain function in health and disease [Cheng et al., 2016; Deco & Kringelbach, 2014]. Here, we go beyond functional connectivity to effective connectivity (EC) between different brain areas to measure directed influences of human brain regions on each other. EC is conceptually very different, for it measures the effect of one brain region on another in a particular direction, and can in principle, therefore, provide information more closely related to the causal processes that operate in brain function, that is, how one brain region influences another. In the context of disorders of brain function, the EC may provide evidence on which brain regions may have altered function, and then influence other brain regions, by comparing EC in individuals with autism and control participants. EC is also more powerful, in that it provides a generative model for brain dynamics—a model that can also generate functional connectivity data features.

In this research, we utilize an approach to the measurement of EC in which each brain area has a simple dynamical model, and known anatomical connectivity is used to provide constraints [Gilson et al., 2018; Gilson, Moreno-Bote, Ponce-Alvarez, Ritter, & Deco, 2016; Rolls et al., 2019; Rolls et al., 2018]. This helps the approach to measure the EC between the 94 automated anatomical atlas (AAL2) [Rolls, Joliot, & Tzourio-Mazoyer, 2015] brain areas using resting-state functional magnetic resonance imaging. (The names of the AAL2 areas are shown in Table S1, and the areas can be viewed with the Mricron viewer.) For this, we used a large number of autistic people and controls and were able to use for this analysis data in a large resting-state fMRI data set, the autism brain imaging data exchange (ABIDE [http://fcon\\_1000.projects.nitrc.org/indi/abide/](http://fcon_1000.projects.nitrc.org/indi/abide/)), which has already proved useful [Di Martino et al., 2014].

## Methods

### *Participants*

The ABIDE repository is hosted by the 1,000 Functional Connectome Project/International Neuroimaging Data-sharing Initiative ([http://fcon\\_1000.projects.nitrc.org](http://fcon_1000.projects.nitrc.org)), and consists of data sets for 1,112 individuals (ABIDE I), comprised of 539 individuals with autism and 573 typically developing controls. All data are fully anonymized in accordance with Health Insurance Portability and Accountability guidelines. All data released were visually

inspected by members of the ABIDE project. Details of diagnostic criteria, acquisition, informed consent, and site-specific protocols are available at [http://fcon\\_1000.projects.nitrc.org/indi/abide/](http://fcon_1000.projects.nitrc.org/indi/abide/).

The inclusion criteria for sample selection include: (a) functional MRI data were successfully preprocessed with manual visual inspection of normalization to MNI space; (b) any data with a mean framewise displacement exceeding 0.5 mm were excluded; (c) subjects were excluded if the percentage of “bad” points (framewise displacement >0.5 mm) was over 0.35 in volume censoring; (d) data collection centers were only included if they have at least 19 individuals and they have the IQ of the individuals recorded. After quality control, a total of 867 subjects (394 people with autism, and 473 controls) met all inclusion criteria. The demographic and clinical characteristics of participants satisfying the inclusion criteria are summarized in Table S2.

### *Effective Connectivity Measurement*

Neuroimaging preprocessing was performed with standard techniques by the Preprocessed Connectomes Project (<http://preprocessed-connectomes-project.github.io/abide/index.html>). No temporal band-pass filtering was applied. This ensures that fast fluctuations in the signal remained available for an efficient connectivity analysis (but the linear drifts in the BOLD signal time series were regressed out to remove any linear trends in the data). After preprocessing, the whole brain (gray matter) was parcellated into 94 regions of interest (ROI) using the AAL2 atlas [Rolls et al., 2015], which includes a useful parcellation of the orbitofrontal cortex. The time series were extracted in each ROI by averaging the signals of all voxels within that region. The names of the ROIs are listed in Table S1.

We used a method that provides efficient calculation of maximum-likelihood EC estimates for a large number (94) of nodes [Gilson et al., 2016, 2018; Rolls et al., 2018, 2019]. The method uses transitions of fMRI measurements across successive repetition times (volumes) and takes into account known anatomical connections. The EC model captures and uses this information via the covariances with nonzero time shifts. Both the EC in the model and the local input variance in a parameter  $\Sigma$  are optimized such that the model best reproduces statistics of the observed fMRI signals. The resting-state analysis described here can be thought of as probing the connectivities between brain regions by analyzing the effects on the system of perturbations produced by noise related to the random spiking times of neurons [Rolls & Deco, 2010]. A description of the EC method follows, and full details of the EC method and statistical analysis are provided in the Supplementary Material.

A classical approach to measuring EC is dynamic causal modeling (DCM) [Bajaj, Adhikari, Friston, & Dhamala, 2016; Friston, 2009; Valdes-Sosa, Roebroeck, Daunizeau, & Friston, 2011]. DCM is often used with circuits consisting of a priori selected brain regions to test hypotheses on the interactions between the considered regions. Here, we instead use a network model with simpler assumptions than those typically used in DCM to perform a large-scale connectivity analysis involving many brain areas [Gilson et al., 2016]. This allows for the very efficient calculation of maximum-likelihood EC estimates for a large number (94) of nodes, individually for a large cohort of participants. In this way, we target significant EC differences for all existing connections (as determined by DTI) that characterize autism with false discovery rate (FDR) correction and without preliminary knowledge, expecting a distributed pattern of abnormal EC links across the brain. Our estimation procedure [Gilson et al., 2016] iteratively optimizes a network model such that it reproduces the empirical cross-covariances between ROIs, which are canonically related to the cross-spectral density used in recent studies that apply DCM to resting-state fMRI data [Friston, Kahan, Biswal, & Razi, 2014; Razi et al., 2017]. Our model uses an exponential approximation of BOLD autocovariance (locally over a few TRs) and discards very slow-frequency fluctuations. Because we are dealing with broadband (slow) fluctuations in neuronal signals, we can simplify our modeling of EC by using an adiabatic approximation (in which we can ignore the effects of the hemodynamic response function) and treat the measured signals as a direct reflection of underlying neuronal activity. Finally, we place positivity constraints on extrinsic or between node connections—in line with known neuroanatomy and previous modeling studies [Marreiros, Kiebel, & Friston, 2008], for the reasons described below. The last simplification compared to DCM includes a fixed (but plausible) form of endogenous neuronal fluctuations ( $\Sigma$ —i.e. sigma in our model) that were characterized by a single (variance) parameter in each region or node. In spite of these differences, we still borrow the term “effective connectivity” from the DCM literature as our connectivity estimates relate to directional interactions between ROIs in the brain network. This model-based approach has been successfully applied to identify changes in the cortical coordination between rest and movie viewing [Gilson et al., 2018], and to EC in depression [Rolls et al., 2018] and in schizophrenia [Rolls et al., 2019].

Compared to DCM the new method used here [Gilson et al., 2016] is computationally more efficient and thus can analyze larger networks because it limits the degrees of freedom for each brain region by utilizing a simpler model of each brain region, and because it uses some structural connectivity information from, for example, diffusion tensor imaging to reduce the number of nodes between which effective connectivity needs to be computed. Furthermore,

the new EC method focuses on transitions between fMRI “activity states” across successive time points [Mitra, Snyder, Tagliazucchi, Laufs, & Raichle, 2015] and does not include details about hemodynamics like the Balloon model [Friston, Mechelli, Turner, & Price, 2000]. The estimated EC measures the strengths of causal interactions from one brain area to another, via the proxy of BOLD fluctuations: it provides a single number that lumps together the effects of the strength of the synapse, and neurotransmitter release, and so forth. The synaptic conductivity interpretation also relates to our earlier neuron-level models in which the synaptic conductivity between modules is a key parameter that specifies how much one module influences another module [Rolls, Webb, & Deco, 2012]. The new method has the additional advantage that each brain region or module has its own  $\Sigma$  parameter, which specifies the variance of the module’s activity, which may be related to the intrinsic excitability of the region. In relation to our integrate-and-fire models, the parameter  $w+$  that defines the strength of the recurrent collateral synapses within the attractor network [Rolls, 2016; Rolls & Deco, 2010; Rolls et al., 2012] may relate to the  $\Sigma$  parameter in the current EC approach [Gilson et al., 2016], because the local feedback influenced by  $w+$  influences the fluctuations of the activity, for example, how readily an area will transition to a high firing rate state. That is, Sigma corresponds in the model to the spontaneous activity (its variance) of a region, and this propagates via the effective connectivities to the other nodes in the recurrent network. A higher value for Sigma relative to controls indicates more fluctuating activity, which could reflect an increase of activity.

The EC model and algorithm used here is closely related to the linearized version of the DCM that is used for the resting state [Frassle et al., 2017; Friston et al., 2014] and for task-related fMRI [Gilson et al., 2018]. Although the hemodynamics of the filtering is modeled for DCM, the complex nonlinearity is simplified in the EC algorithm used here [Gilson et al., 2016], which enables it to be applied to a whole-brain parcellation with many nodes (in this case, the 94 nodes of the AAL2 atlas). Instead of the model comparison used by DCM to find the best network topology, the current algorithm uses structural data (from DTI) to specify possible connections in the model, thereby simplifying the operation of the model because some links with no known anatomical connection are excluded. (However, the algorithm settles similarly in practice with typical fMRI data even when these anatomical constraints are removed.) The implication is that significant differences of EC identified with this algorithm (here autism vs. controls) are expected to reflect significant changes in the corresponding DCM. The results were thresholded at  $P < 0.05$ , correcting multiple comparisons using the FDR ( $q < 0.05$ ).

Forward versus backward EC: The connections between adjacent cortical areas in a sensory hierarchy can usually

be classified as forward (from the sensory input) versus backward (from an upper region in the hierarchy to the preceding region) [Rolls, 2016]. Forward connectivity is often characterized by connections from layer 2–3 pyramidal cells forwards to layers 4, and 2 and 3, of the next cortical area. Back projections between adjacent cortical areas in a hierarchy typically arise from the deep layers of the cerebral cortex, mainly layer 5, and project back mainly to layer 1 of the preceding cortical area [Markov et al., 2013, 2014; Markov & Kennedy, 2013; Markov et al., 2014; Rolls, 2016]. Given the termination on the apical dendrites in layer 1, far from the cell bodies, the backward projections are generally found to be modulatory or weaker, relative to driving forward connections, with effects reducing the back projecting efficacy including shunting on the dendrites produced by other inputs to pyramidal cells. It is also crucial for attention and memory recall that the top-down or back projections are weaker than the forward connections, so that attentional biasing and memory recall does not dominate over bottom-up forward inputs [Deco & Rolls, 2005; Fuster, 2015; Rolls, 2016; Rolls & Deco, 2002; Turova & Rolls, 2019]. In areas of the brain apart from sensory hierarchies, there may also be similar asymmetries for systems-level functional reasons, for example, that short-term memory processing in prefrontal cortical areas does not dominate perceptual processing in the temporal and parietal areas that utilize the prefrontal cortex for short-term memory [Goldman-Rakic, 1996]. Because this asymmetry of the strength of the connectivity between brain regions is so important functionally, and usually has an anatomical basis, we conceptualize some of the effective connectivities analyzed in this investigation as forward or backward based on the strengths in each direction, as well as information about the anatomy of the different brain areas being connected [Rolls, 2016]. It is at the same time the case that the effective connectivities can change to some extent based on whether sensory inputs versus memory recall (for example) are being performed, but nevertheless, the forward and backward connectivity difference between many brain areas is large (as shown in the Results). In this article, we refer to the strengths of the connectivities in each direction as “stronger direction” or “weaker direction,” but the concepts in this paragraph provide some insight into how this may relate to cortical structure and function [Rolls, 2016].

### *Clinical Correlates*

We also investigated whether differences in EC among individuals with autism were correlated with symptoms assessed by the Autism Diagnostic Observational Schedule (ADOS) total, communication, social and stereotyped behavior scores. We used the Liptak–Stouffer z-score method [Liptak, 1958] to combine the data from the

different neuroimaging sites for this analysis, for this provides a principled way to take into consideration possible differences in these measures between sites. Specifically, we calculated the partial correlation between the normalized effective connectivities and the clinical scores, with head motion, age, sex and IQ as covariates so that they did not contribute to the correlation between the ECs and the clinical scores, in each individual center. Then we used the Liptak–Stouffer z-score method to combine the results from the individual data sets [Liptak, 1958].

## **Results**

### *Differences of Effective Connectivity between Individuals with Autism and Controls*

Table 1 shows the top 41 links with the most significant differences in EC between individuals with autism and controls. Links are considered here if there was a significant difference for a link between individuals with autism and controls using FDR correction for multiple comparisons ( $P < 0.05$ ), for which the significance level must be  $P < 0.00081$ . (In addition, to focus on links with a reasonable strength of EC that is likely to be meaningful in value [Rolls et al., 2019; Rolls et al., 2018] as well as significantly different in autism, links are shown if their EC value in either direction exceeds the threshold of 0.02 Hz.) Figure 1 shows similar information in diagrammatic form and includes all links that satisfy the two criteria just described. Figure 2A shows these links between AAL2 nodes shown on views of the brain. Figure 2B shows the main areas with on average increases or decreases in their EC directed to or from them in autism.

We now describe some of the main changes in EC in autism, using the summaries in Tables 2 and 3, and also illustrated in Figure 3. Table 2 summarizes links *from* a brain region (region 1) that have different EC in autism, and Table 3 summarizes links *to* a brain region (region 2) that have different EC in autism. In addition, in Tables 2 and 3 we indicate for the ECs, the stronger direction as *S* defined as the direction in which the EC from Region 1 to Region 2 is stronger in the controls; *W* as the direction in which the EC is weaker from region 1 to region 2; and *Bid* (bidirectional) in which the ECs between Region 1 and Region 2 are similar. We note that all the information in Tables 2 and 3 are from the 41 links shown in Table 1.

First, the middle temporal gyrus (Temporal\_Mid) and some other temporal cortical areas have lower EC to the precuneus and cuneus in the ASD group, as summarized in Table 3. These effective connectivities are in the stronger direction. In addition, the Temporal Pole has lower EC to FrontalMedOrb, which is the VMPFC BA 10, and these are in the stronger direction. In addition, there is an EC link from the middle temporal gyrus to the hippocampus that is increased, and this is the stronger direction (Table 1). Thus, the pattern for the temporal cortex in

**Table 1. Effective Connectivity (EC) Links That Are Different Between Individuals With Autism and Controls**

| Region1AAL2 name               | Region2AAL2 name        | z value (1-2) | P value (1-2) | z value (2-1) | P value (2-1) | EC in HC (1-2) | EC in AUT (1-2) | EC in HC (2-1) | EC in AUT (2-1) | EC ratio in HC (strong/weak) |
|--------------------------------|-------------------------|---------------|---------------|---------------|---------------|----------------|-----------------|----------------|-----------------|------------------------------|
| Temporal_Mid_R                 | Cuneus_R (S)            | -5.556        | 2.76e-08*     | -3.222        | 1.27E-03      | 0.031          | 0.029           | 0.010          | 0.010           | 3.077                        |
| Temporal_Mid_L                 | Cuneus_L (S)            | -5.092        | 3.54e-07*     | -3.031        | 2.44E-03      | 0.040          | 0.030           | 0.011          | 0.010           | 3.630                        |
| Paracentral_Lobule_R           | Postcentral_L (W)       | -4.836        | 1.32e-06*     | -2.125        | 3.36E-02      | 0.027          | 0.021           | 0.066          | 0.070           | 2.453                        |
| Temporal_Mid_L                 | Hippocampus_L (S)       | 4.449         | 8.65e-06*     | 4.244         | 2.20e-05*     | 0.021          | 0.029           | 0.017          | 0.022           | 1.228                        |
| Temporal_Mid_L                 | Cuneus_R (S)            | -4.411        | 1.03e-05*     | -3.274        | 1.06E-03      | 0.025          | 0.023           | 0.009          | 0.009           | 2.789                        |
| Temporal_Mid_R                 | Lingual_R (S)           | -4.327        | 1.51e-05*     | -1.738        | 8.22E-02      | 0.033          | 0.028           | 0.016          | 0.015           | 2.142                        |
| Hippocampus_L Frontal_L        | Mid_L (W)               | 4.244         | 2.20e-05*     | 4.449         | 8.65e-06*     | 0.017          | 0.022           | 0.021          | 0.029           | 1.228                        |
| Sup_Medial_R                   | Sup_2_L (W)             | -4.187        | 2.83e-05*     | -1.548        | 1.22E-01      | 0.033          | 0.030           | 0.038          | 0.036           | 1.136                        |
| Putamen_R                      | Postcentral_R (S)       | 4.040         | 5.35e-05*     | 1.439         | 1.50E-01      | 0.030          | 0.038           | 0.016          | 0.020           | 1.901                        |
| Paracentral_Lobule_R           | Precentral_R (W)        | -4.025        | 5.71e-05*     | -1.473        | 1.41E-01      | 0.027          | 0.023           | 0.085          | 0.090           | 3.121                        |
| ParaHippocampal_L              | Calcarine_L (S)         | -3.930        | 8.48e-05*     | -0.415        | 6.78E-01      | 0.041          | 0.044           | 0.016          | 0.015           | 2.532                        |
| Putamen_R                      | Lobule_R (S)            | 3.865         | 1.11e-04*     | 0.997         | 3.19E-01      | 0.025          | 0.033           | 0.009          | 0.011           | 2.671                        |
| Thalamus_L                     | Sup_L (S)               | 3.855         | 1.16e-04*     | 2.759         | 5.80E-03      | 0.022          | 0.028           | 0.022          | 0.027           | 1.018                        |
| Hippocampus_L Temporal_Mid_L   | Inf_L (W)               | 3.822         | 1.32e-04*     | 3.004         | 2.67E-03      | 0.016          | 0.023           | 0.025          | 0.030           | 1.603                        |
| ParaHippocampal_R              | Postcentral_L (S)       | -3.804        | 1.42e-04*     | -1.614        | 1.07E-01      | 0.024          | 0.023           | 0.020          | 0.021           | 1.186                        |
| Frontal_Caudate_L              | Calcarine_R (S)         | -3.794        | 1.48e-04*     | -0.092        | 9.27E-01      | 0.033          | 0.032           | 0.017          | 0.021           | 1.956                        |
| ParaHippocampal_R Frontal_L    | Inf_Orb_2_L (S)         | 3.745         | 1.81e-04*     | 2.302         | 2.13E-02      | 0.023          | 0.030           | 0.012          | 0.014           | 1.910                        |
| Sup_Medial_L                   | Lingual_R (S)           | -3.739        | 1.85e-04*     | -1.104        | 2.70E-01      | 0.049          | 0.046           | 0.018          | 0.021           | 2.655                        |
| Amygdala_L                     | Frontal_Mid_2_R (W)     | 3.709         | 2.08e-04*     | 1.960         | 5.01E-02      | 0.009          | 0.014           | 0.024          | 0.028           | 2.744                        |
| Temporal_Mid_R                 | Temporal_Mid_L (W)      | 3.687         | 2.27e-04*     | 3.349         | 8.10E-04      | 0.015          | 0.018           | 0.034          | 0.048           | 2.271                        |
| Parietal_Sup_R                 | Precuneus_L (S)         | -3.682        | 2.31e-04*     | 0.974         | 3.30E-01      | 0.059          | 0.053           | 0.009          | 0.010           | 6.616                        |
| Putamen_R                      | Cuneus_R (S)            | -3.645        | 2.67e-04*     | -1.079        | 2.81E-01      | 0.024          | 0.027           | 0.021          | 0.031           | 1.146                        |
| Thalamus_R                     | Precentral_R (S)        | 3.627         | 2.87e-04*     | -0.013        | 9.90E-01      | 0.034          | 0.043           | 0.022          | 0.026           | 1.511                        |
| Precentral_L Frontal_Sup_2_L   | Fusiform_R (W)          | 3.610         | 3.06e-04*     | 1.411         | 1.58E-01      | 0.013          | 0.019           | 0.026          | 0.035           | 1.974                        |
| Temporal_Pole_Mid_R            | Supp_Motor_Area_L (S)   | -3.608        | 3.09e-04*     | -1.287        | 1.98E-01      | 0.071          | 0.069           | 0.034          | 0.035           | 2.101                        |
| Paracentral_Lobule_R           | Frontal_Mid_2_R (W)     | 3.604         | 3.14e-04*     | 2.121         | 3.39E-02      | 0.016          | 0.025           | 0.023          | 0.029           | 1.474                        |
| Temporal_Pole_Mid_R            | Cuneus_R (S)            | -3.599        | 3.20e-04*     | -2.627        | 8.61E-03      | 0.023          | 0.021           | 0.008          | 0.007           | 2.971                        |
| Thalamus_L Temporal_Pole_Mid_R | Postcentral_R (W)       | -3.595        | 3.24e-04*     | -0.390        | 6.96E-01      | 0.031          | 0.027           | 0.067          | 0.072           | 2.158                        |
| Hippocampus_R Pallidum_L       | Frontal_Med_Orb_R (S)   | -3.576        | 3.49e-04*     | -2.003        | 4.52E-02      | 0.055          | 0.049           | 0.022          | 0.022           | 2.439                        |
| Thalamus_L Temporal_Pole_Mid_R | Frontal_Inf_Orb_2_L (S) | 3.560         | 3.71e-04*     | 1.645         | 1.00E-01      | 0.020          | 0.028           | 0.015          | 0.017           | 1.379                        |
| Hippocampus_R Pallidum_L       | Lingual_R (S)           | -3.556        | 3.77e-04*     | -2.004        | 4.51E-02      | 0.035          | 0.031           | 0.012          | 0.012           | 2.863                        |
| Hippocampus_R Pallidum_L       | Temporal_Mid_R (W)      | 3.543         | 3.96e-04*     | 1.220         | 2.23E-01      | 0.018          | 0.024           | 0.020          | 0.023           | 1.120                        |
| Hippocampus_R Pallidum_L       | Postcentral_L (S)       | 3.483         | 4.96e-04*     | 2.269         | 2.33E-02      | 0.020          | 0.029           | 0.017          | 0.022           | 1.177                        |

*(Continues)*

**Table 1. Continued**

| Region1AAL2 name     | Region2AAL2 name    | z value (1-2) | P value (1-2) | z value (2-1) | P value (2-1) | EC in HC (1-2) | EC in AUT (1-2) | EC in HC (2-1) | EC in AUT (2-1) | EC ratio in HC (strong/weak) |
|----------------------|---------------------|---------------|---------------|---------------|---------------|----------------|-----------------|----------------|-----------------|------------------------------|
| Occipital_Inf_L      | Occipital_Inf_R (S) | -3.482        | 4.98e-04*     | -1.180        | 2.38E-01      | 0.083          | 0.077           | 0.065          | 0.068           | 1.268                        |
| Temporal_Mid_R       | Heschl_R (S)        | -3.447        | 5.68e-04*     | -2.057        | 3.97E-02      | 0.036          | 0.030           | 0.021          | 0.021           | 1.691                        |
| Putamen_L            | Cingulate_Mid_R (S) | 3.432         | 6.00e-04*     | -1.298        | 1.94E-01      | 0.028          | 0.038           | 0.024          | 0.025           | 1.201                        |
| SupraMarginal_L      | SupraMarginal_R (S) | -3.425        | 6.15e-04*     | -2.133        | 3.30E-02      | 0.090          | 0.094           | 0.081          | 0.084           | 1.105                        |
| Frontal_Sup_2_L      | Frontal_Mid_2_L (W) | 3.413         | 6.42e-04*     | 0.898         | 3.69E-01      | 0.054          | 0.064           | 0.064          | 0.069           | 1.187                        |
| Frontal_Sup_Medial_R | Olfactory_R (W)     | 3.402         | 6.70e-04*     | 0.729         | 4.66E-01      | 0.016          | 0.021           | 0.024          | 0.025           | 1.512                        |
| Putamen_L            | Cingulate_Mid_L (S) | 3.377         | 7.34e-04*     | -0.525        | 6.00E-01      | 0.033          | 0.043           | 0.020          | 0.020           | 1.669                        |
| Putamen_L            | Temporal_Sup_L (S)  | 3.359         | 7.82e-04*     | 1.809         | 7.05E-02      | 0.042          | 0.054           | 0.020          | 0.023           | 2.125                        |

Links are shown if their EC value in either direction exceeds the threshold of 0.02 Hz, and if there is a significant difference using FDR correction for multiple comparisons between individuals with autism and controls, for which the significance level must be  $P < 0.00081$ . A negative value for z indicates a lower effective connectivity link in individuals with autism. All 41 links with these EC differences are shown. (“\*” indicates this direction is significant; “Strong/Weak” indicates the ratio of the EC from 1 to 2 in terms of the strong direction/the weak direction.)

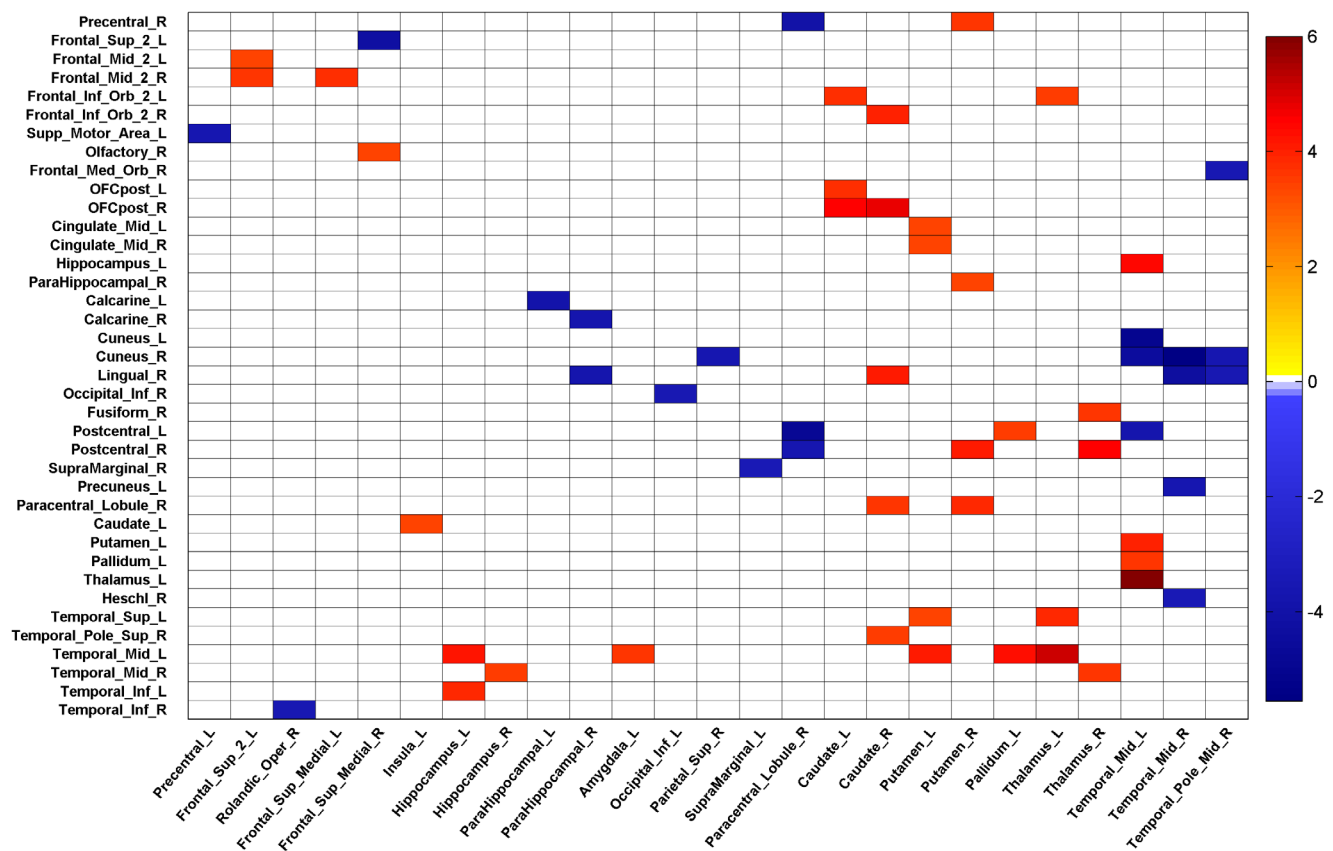


**Figure 1.** The matrices of differences in effective connectivity between individuals with autism and controls. The axes are the AAL2 areas, shown in their numbered order and with their names in Table S1. The effective connectivity matrix has the index  $j$  for the columns and the index  $i$  for the rows. The matrix is thus nonsymmetric, and the effective connectivity is always from  $j$  to  $i$ . The effective connectivity between any pair of links is shown in one direction in the upper right of the matrix and in the opposite direction in the lower left. The table includes only AAL2 areas between which there is a significant difference in effective connectivity.

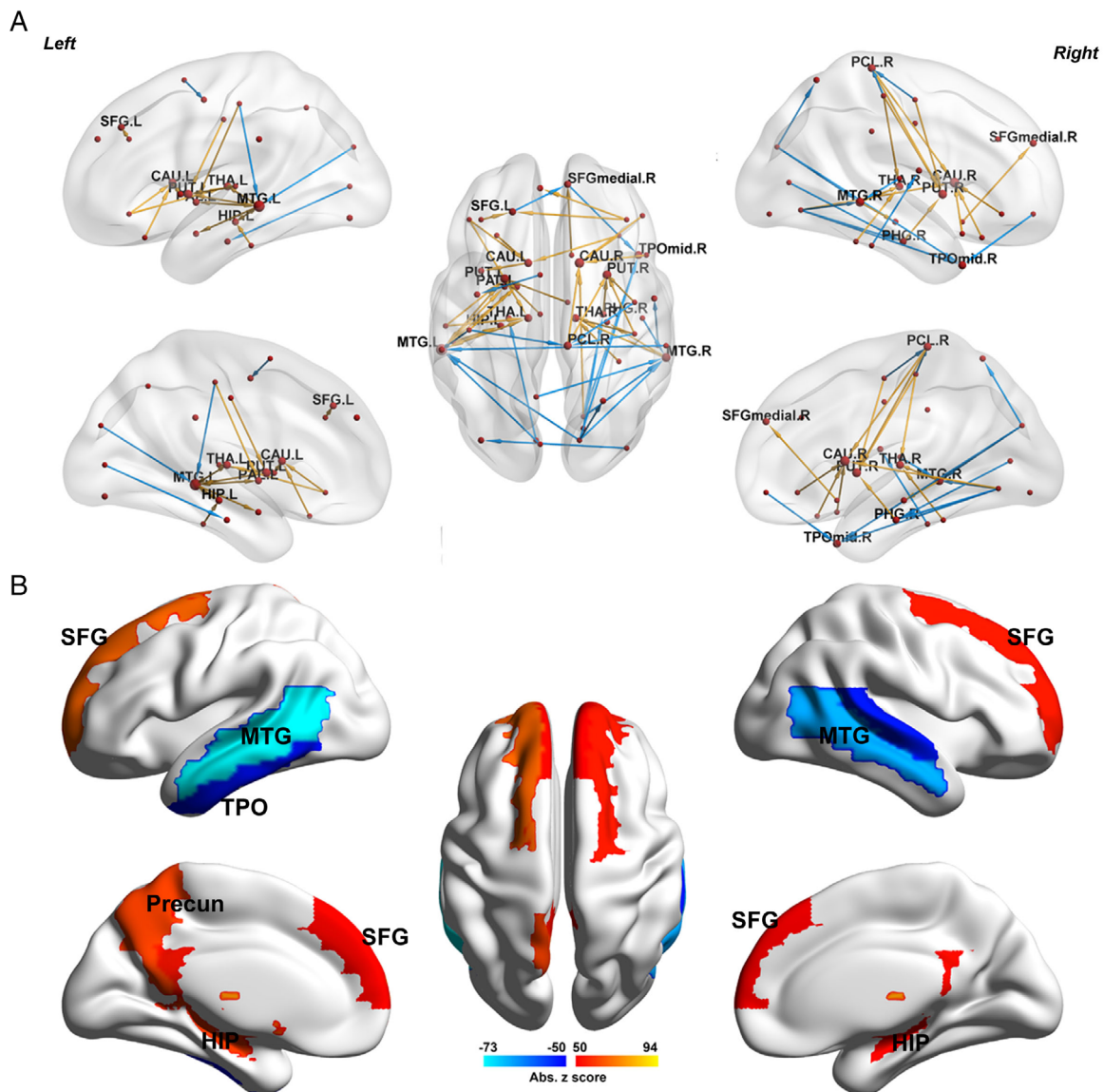


**Figure 2.** (A) Differences in effective connectivity between individuals with autism and controls. The links shown are those with significantly different effective connectivity after FDR  $P < 0.05$  correction. Red indicates that the effective connectivity is increased in individuals with autism, and blue that it is decreased. There were 41 such links significant with FDR correction,  $P < 0.05$ , and with effective connectivity values in at least one direction that were greater than 0.02 Hz. The glass brains were generated using the BrainNet Viewer [Xia, Wang, & He, 2013]. (B) The AAL2 atlas areas with effective connectivities those were significantly different in individuals with autism. An area is shown if it has effective connectivities either from it or to it that are different in autism.

autism is decreased EC to the precuneus and cuneus, and to the VMPFC; and increased EC to the hippocampus.

Second, the hippocampus and amygdala have increased EC to the middle temporal gyrus in autism, and this is mainly in the weaker direction (with the macaque neuroanatomy providing evidence that these are back projections [Amaral & Price, 1984; Lavenex & Amaral, 2000; Rolls, 2016; Van Hoesen, 1982]), though there is also an increase in the stronger direction (Tables 1, 2, and 3). (In addition, the parahippocampal gyrus has decreased EC to early visual cortical areas such as the calcarine cortex in autism.)

Third, some frontal cortical areas (FrontalSup and Supmedial) have increased EC to the middle frontal gyrus and decreased EC to the superior frontal gyrus.

#### *Correlation between the Effective Connectivities and the Autism Symptom Scores*

The correlations of the effective connectivities with the autism symptom scores are shown in Table S5 and Table S4. The ECs from the middle temporal gyrus to the precuneus were negatively correlated with the ADOS total, communication, and

**Table 2. Summary of the Main Differences in Effective Connectivity (EC) From One Brain Region (1) To Other Brain Regions (2) in Autism**

| Region 1                    | Region 2 (a set of regions)   | z value of region 1–2 EC | z value of region 2–1 EC | EC of region 1–2 in HC | EC of region 1–2 in AUT | EC of region 2–1 in HC | EC of region 2–1 in AUT |
|-----------------------------|---|--------------------------|--------------------------|------------------------|-------------------------|------------------------|-------------------------|
| Temporal                    | Hippocampus_L (S),<br>Heschl_R (Bid), Post_central_L (Bid),<br>Cuneus_R (S), Cuneus_L(S), Precuneus_L (S),<br>Lingual_R(S), Frontal_Med_Orb_R (S),<br>Temporal_Mid_L (Bid), Temporal_Mid_R,<br>(Bid) Temporal_Inf_L (W) | 4.448                    | 4.244                    | 0.021                  | 0.029                   | 0.017                  | 0.022                   |
|                             |   | −4.105                   | −2.060                   | 0.036                  | 0.032                   | 0.014                  | 0.014                   |
|                             |   | 3.870                    | 2.891                    | 0.017                  | 0.023                   | 0.022                  | 0.027                   |
| Hippocampus                 |   | 3.687                    | 3.349                    | 0.015                  | 0.018                   | 0.034                  | 0.048                   |
| Amygdala                    |   | −3.821                   | −0.537                   | 0.041                  | 0.041                   | 0.017                  | 0.019                   |
| Parahippocampal             | Lingual_R (S), Calcarine_L (S), Calcarine_R (S)<br>Frontal_Mid_2_L (W), Frontal_Mid_2_R (W),<br>Olfactory_R (W)   | 3.532                    | 1.427                    | 0.023                  | 0.031                   | 0.034                  | 0.038                   |
| FrontalSup and<br>SupMedial | Frontal_Sup_2_L (Bid),  | −4.187                   | −1.548                   | 0.033                  | 0.030                   | 0.038                  | 0.036                   |

A positive value for z indicates a higher EC in autism (AUT). Each link is followed by S if it is in the Strong direction; by W if it is in the Weak direction; and by Bid if the EC is similar in both directions.

social score (Table S5). Thus the weaker this EC value the greater was the autism score, in line with the finding that the ECs from the temporal cortex to the precuneus were decreased in autism (Tables 1, 2, and 3).

The ECs from the hippocampus to the temporal cortex were positively correlated with the ADOS stereotyped behavior score (Table S5). Thus the stronger the EC value the greater was the autism score, in line with the finding that the ECs from the hippocampus to the temporal cortex were increased in autism (Tables 1, 2, and 3).

#### Differences in Sigma in Autism

Sigma (i.e.,  $\Sigma$ —the amplitude of endogenous neuronal fluctuations) was lower in the VMPFC (BA 10) in the group with autism ( $z = -4.12$ ,  $P = 3.8e-5$ ). This implies less activity in the VMPFC in people with autism.

#### Comparison with Functional Connectivity

For completeness, the functional connectivity differences between participants with autism and controls found in the same data set and using the AAL2 parcellation are

shown in Table S3. (This is different from our previous work, which was a voxel-level study, and was with a somewhat larger group of participants [Cheng et al., 2015].) It will be seen that only some of the areas with different functional connectivity have significantly different EC, and this is to be expected, as they measure different properties of the connectivity. It is also of interest that all the top 25 functional connectivities (those significant after Bonferroni correction  $P < 0.05$ ) were lower in autism than in controls (Table S3), whereas for the effective connectivities, some higher effective connectivities were found (Fig. 1). With FDR correction ( $P < 0.05$ ), 836 functional connectivity links were significantly different in autism, and of these 825 were lower in autism. This is of interest, for this elucidates one way in which effective connectivities can provide information that is not available from the functional connectivities.

**Robustness of the EC results.** The results described here were with a relatively large data set of 394 people with ASD and 473 controls and should be robust with this sample size. However, as a check on whether similar

**Table 3. Summary of the Main Differences in Effective Connectivity (EC) To One Brain Region (2) From Other Brain Regions (1) in Autism**

| Region 1 (a set of regions)   | Region 2        | z value of region 1–2 EC | z value of region 2–1 EC | EC of region 1–2 in HC | EC of region 1–2 in AUT | EC of region 2–1 in HC | EC of region 2–1 in AUT |
|---|-----------------|--------------------------|--------------------------|------------------------|-------------------------|------------------------|-------------------------|
| Temporal_Mid_L (S), Temporal_Mid_R (S),<br>Temporal_Pole_Mid_R (S), Parietal_Sup_R (Bid)    | Cuneus          | −4.461                   | −2.647                   | 0.029                  | 0.026                   | 0.012                  | 0.013                   |
| Caudate_L(S), Thalamus_L(S)   | FrontalInfOrb_L | 3.652                    | 1.974                    | 0.021                  | 0.029                   | 0.013                  | 0.016                   |
| Temporal_Pole_Mid_R (S)   | FrontalMedOr_R  | −3.576                   | −2.003                   | 0.055                  | 0.049                   | 0.022                  | 0.022                   |
| Frontal_Sup_2_L (W), Frontal_Sup_Medial_L (W)   | FrontalMid      | 3.576                    | 1.660                    | 0.026                  | 0.034                   | 0.037                  | 0.042                   |
| Temporal_Mid_R (S),<br>Amygdala_L (W), Hippocampus (Bid),<br>Putamen_L (S), Thalamus_L(Bid) | Precuneus       | −3.682                   | 0.974                    | 0.059                  | 0.053                   | 0.009                  | 0.010                   |
|   | Temporal        | 3.752                    | 2.765                    | 0.022                  | 0.028                   | 0.024                  | 0.030                   |

A positive value for z indicates a higher EC in autism (AUT). Entries in Tables 2 and 3 are not mutually exclusive.

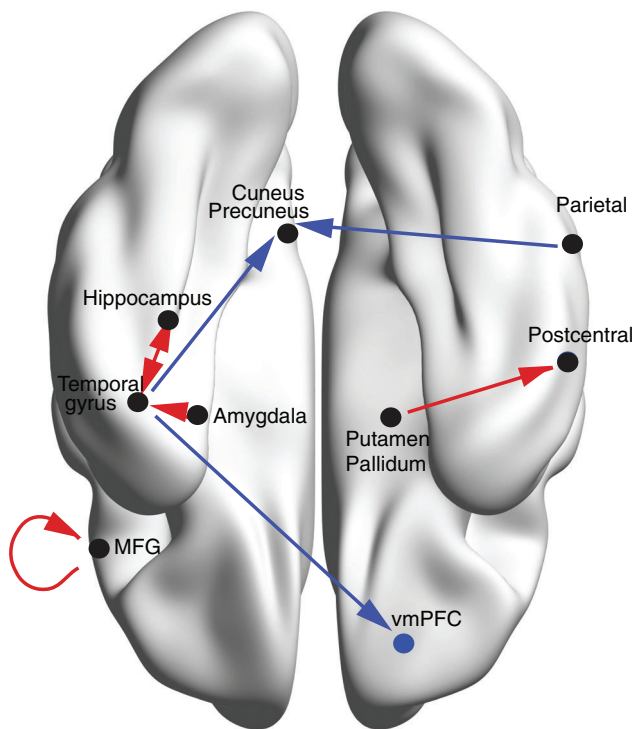


**Figure 3.** Summary of some of the main changes in Effective Connectivity in autism. The increased effective connectivities in autism are shown in red, and decreased in blue. A blue circle indicates a decrease in Sigma in autism. For details of the effective connectivities, see Tables 1, 2, and 3 and Figure 1.

results would be obtained with a smaller sample as a form of internal validation, we performed a split data analysis, in which the autism and control group were split into independent data sets. From the ABIDE1 data set from which data from 16 neuroimaging sites were used in the main analyses, the data from eight neuroimaging sites formed one data split, and from the other eight sites the second data split. The numbers of participants in each split were similar. Overall, for the results shown in Tables 1, 2, and 3, consistent results were found in each of the two data splits, with the correlations with the presented results (of the  $t$  values of the differences of all ECs between the autism and control groups) 0.83 for the first split, and 0.78 for the second split. Furthermore, most of the EC links with significant differences in the whole data set were also significant ( $P < 0.05$ ) in both of the split data sets (67/80). Furthermore, all the significant differences in EC between the autism and control groups shown in Figure 3 were also significant in each of the two data splits, apart from two, which were significant in one of the data splits. These analyses confirm the robustness of the results presented here with the full data set; but also make the point that large sample sizes are needed for resting-state connectivity analyses to obtain robust results.

## Discussion

Figure 3 summarizes some of the differences in EC in autism found in this investigation, with further details in Tables 1, 2, and 3. These differences are discussed next.

First, the middle temporal gyrus (Temporal\_Mid) and some other temporal cortical areas have decreased ECs to the precuneus and cuneus (Tables 1, 2, and 3), and these are correlated with the ADOS total, communication, and social score (Table S5). These findings are supported by the decrease in functional connectivity between these areas described previously [Cheng et al., 2015], but the new findings provide evidence on the directionality of the effect, with the EC in the reverse direction from the precuneus to the temporal lobe being both very much weaker, and less significantly different between people with autism and controls (Table 2). This is important new evidence. These temporal lobe areas, especially the parts of the middle temporal gyrus identified in the voxel-level functional connectivity study, are implicated in face expression analysis and in theory of mind [Cheng et al., 2015; Critchley et al., 2000; Hasselmo, Rolls, & Baylis, 1989]. Furthermore, in autism poor face recognition performance predicted smaller activation in the right anterior temporal lobe to faces [Scherf, Elbich, Minshew, & Behrmann, 2015], further implicating these temporal lobe areas in the problems in face processing in autism [Deutsch & Raffaele, 2019]. The precuneus and cuneus regions are implicated in the sense of self, in autobiographical memory retrieval, and of spatial processing that is relevant to that [Cavanna & Trimble, 2006; Fretton et al., 2014; Hirshhorn, Grady, Rosenbaum, Winocur, & Moscovitch, 2012]. The implication of the new EC results is that the facial expression analysis, which is important in social interactions, and theory of mind, important in understanding others' behavior, have reduced effects in autism on parts of the brain involved in representing the self in the world. Thus, this reduced EC from temporal cortex areas to the precuneus and cuneus may be related to the poor understanding of the implications of face expression inputs for oneself in autism.

Another interesting decreased EC is from the temporal cortex (Mid-Pole) to the VMPFC, which latter is implicated in reward evaluation, emotion, and decision-making [Du et al., 2019; Rolls, 2014, 2018a, 2019a, 2019b, 2019c]. This may be related to poor reward and punishment decoding of face expression, and thus to difficulty with social behavior. Interestingly, the sigma value for this VMPFC region, reflecting in the EC analysis the signal variance value Sigma, was lower for autistic people compared to controls. This may reflect reduced processing in the VMPFC if there is reduced input from facial expression and theory of mind middle temporal gyrus areas. This VMPFC region has been reported to be more active in response to self- compared with other-

referential processing, with this difference attenuated in people with autism [Lombardo et al., 2010], further implicating this VMPFC area in autism.

Second, the hippocampus and amygdala have increased EC to the middle temporal gyrus in autism, and this is mainly in the weaker direction (with the macaque neuroanatomy providing evidence that these are back projections [Amaral & Price, 1984; Lavenex & Amaral, 2000; Rolls, 2016; Van Hoesen, 1982]), though there is also an increase in the stronger direction (Tables 1, 2, and 3), and this increase is positively correlated with the ADOS stereotyped behavior score (Table S5). The usual understanding of the connections from the hippocampus back to neocortex is that they are back projections involved in episodic memory retrieval [Kesner & Rolls, 2015; Rolls, 2016, 2018b; Rolls & Wirth, 2018; Treves & Rolls, 1994]. The usual understanding of the connections from the amygdala to the neocortex is that they are back projections [Amaral & Price, 1984], which might be involved in retrieving emotion-related memories [Rolls, 2014, 2016]. An implication is that the increased EC in these pathways may be related to increased retrieval of recent and emotional memories in autism, which may contribute to the state if these are unpleasant memories. In addition, the increased top-down effects from the amygdala and hippocampus on the temporal cortical areas may contribute to the reduced activations of temporal cortex areas to bottom-up inputs produced by faces [Hadjikhani, Joseph, Snyder, & Tager-Flusberg, 2007; Koshino et al., 2008; Pierce, Muller, Ambrose, Allen, & Courchesne, 2001].

Third, some frontal cortical areas (FrontalSup and FrontalSupMedial) have increased EC to the middle frontal gyrus and decreased EC to the superior frontal gyrus. From our functional connectivity study, we know that some of these prefrontal cortex areas have increased functional connectivity with the precuneus and cuneus [Cheng et al., 2015]. Given that the prefrontal cortex is implicated in executive functions, working memory, and planning [Passingham & Wise, 2012], the alterations in EC in these prefrontal cortex areas may be related to increased executive function devoted to the precuneus and cuneus in trying to make sense of the self in the world. They may also relate to the increased spatial processing in which many people with autism excel. Also of potential interest is that activations in the precuneus and posterior cingulate cortex were found to be greater to the faces of familiar people compared to strangers and that this activation was reduced in people with autism [Pierce, Haist, Sedaghat, & Courchesne, 2004]. In the same study, activation to familiar faces was reported to be greater in medial prefrontal cortex areas than in people with autism [Pierce et al., 2004].

We also note that some subcortical effects on cortical areas involved in touch and movement are increased, for example, from the thalamus and putamen to precentral,

postcentral, and midcingulate cortex (Table 1). Autistics are oversensitive to being touched [Lundqvist, 2015; Riquelme, Hatem, & Montoya, 2016]. These increased effective connectivities may be related to this.

In the results described, there were 347 males and 47 females in the autistic group (Table S2), consistent with the increased prevalence of ASDs in males, and the effects of sex were regressed out. If the analysis was restricted to only males in the autism and control groups, then some of the main differences in EC described here remained, including reduced EC from the middle temporal gyrus to the cuneus and precuneus, and increased EC from the amygdala and hippocampus to the middle temporal gyrus. The female-only groups were insufficiently large to obtain FDR-corrected significant differences in EC.

It would be of interest in future investigations to analyze whether subtypes of EC in autism could be found, and to investigate these differences in an even larger group of females and in people with a wider range of age. Furthermore, as EC is an approach to causal analysis, it would be of interest in future studies to investigate possible associations between genes and the differences in EC described here. The present findings make a significant step toward causality, by going beyond functional connectivity, which reflects correlations, to EC, which reflects directed effects of one brain region on another.

In conclusion, this is the first large-scale study of EC in people with autism. The investigation provided important new evidence on directed connectivity in autism, which help to reveal the underlying differences in connectivity in people with autism. One new set of findings was that directed connectivity *from* the middle temporal gyrus areas implicated in face expression processing and theory of mind *to* the precuneus and cuneus implicated in processing about the self was reduced; and that connectivity *from* these middle temporal gyrus areas *to* the VMPFC, involved in emotion and emotion-related decision-making [Rolls, 2019b], was reduced in autism. Another set of findings was that EC *from* memory and emotion-related areas, the hippocampus and amygdala respectively, *to* the middle temporal gyrus was increased in autism. Another set of findings was that EC *from* the basal ganglia *to* the precentral and postcentral gyrus and midcingulate cortex was increased in people with autism.

## Acknowledgments

We acknowledge the use of the ABIDE data set. J.F. is partially supported by the key project of Shanghai Science & Technology Innovation Plan (Nos. 15JC1400101 and 16JC1420402) and the National Natural Science Foundation of China (Grant Nos. 71661167002 and 91630314). The research was also partially supported by the Shanghai AI Platform for Diagnosis and Treatment of Brain Diseases (No. 2016-17). The research was also partially

supported by Base for Introducing Talents of Discipline to Universities No. B18015. W.C. is supported by grants from the National Natural Sciences Foundation of China (Nos. 81701773 and 11771010), and sponsored by the Shanghai Sailing Program (No. 17YF1426200) and the Research Fund for the Doctoral Program of Higher Education of China (No. 2017M610226). W.C. is also sponsored by the Natural Science Foundation of Shanghai (No. 18ZR1404400). The effective connectivity algorithm work was supported by the Human Brain Project (Grant Nos. FP7-FET-ICT-604102 and H2020-720270 HBP SGA1 to G.D.) and the Marie Skłodowska-Curie Action (Grant H2020-MSCA-656547 to M.G.).

## Conflict of Interest

The authors declare that they have no conflict of interest related to this work.

## References

- Amaral, D. G., & Price, J. L. (1984). Amygdalo-cortical projections in the monkey (*Macaca fascicularis*). *Journal of Comparative Neurology*, 230(4), 465–496. <https://doi.org/10.1002/cne.902300402>
- Bajaj, S., Adhikari, B. M., Friston, K. J., & Dhamala, M. (2016). Bridging the gap: Dynamic causal modeling and granger causality analysis of resting state functional magnetic resonance imaging. *Brain Connectivity*, 6(8), 652–661. <https://doi.org/10.1089/brain.2016.0422>
- Cavanna, A. E., & Trimble, M. R. (2006). The precuneus: A review of its functional anatomy and behavioural correlates. *Brain*, 129(Pt 3), 564–583. <https://doi.org/10.1093/brain/awl004>
- Cheng, W., Rolls, E. T., Gu, H., Zhang, J., & Feng, J. (2015). Autism: Reduced functional connectivity between cortical areas involved in face expression, theory of mind, and the sense of self. *Brain*, 138, 1382–1393.
- Cheng, W., Rolls, E. T., Qiu, J., Liu, W., Tang, Y., Huang, C. C., ... Feng, J. (2016). Medial reward and lateral non-reward orbitofrontal cortex circuits change in opposite directions in depression. *Brain*, 139(Pt 12), 3296–3309. <https://doi.org/10.1093/brain/aww255>
- Critchley, H., Daly, E., Phillips, M., Brammer, M., Bullmore, E., Williams, S., ... Murphy, D. (2000). Explicit and implicit neural mechanisms for processing of social information from facial expressions: A functional magnetic resonance imaging study. *Human Brain Mapping*, 9(2), 93–105.
- Deco, G., & Kringelbach, M. L. (2014). Great expectations: Using whole-brain computational connectomics for understanding neuropsychiatric disorders. *Neuron*, 84(5), 892–905. <https://doi.org/10.1016/j.neuron.2014.08.034>
- Deco, G., & Rolls, E. T. (2005). Neurodynamics of biased competition and co-operation for attention: A model with spiking neurons. *Journal of Neurophysiology*, 94, 295–313.
- Deutsch, S. I., & Raffaele, C. T. (2019). Understanding facial expressivity in autism spectrum disorder: An inside out review of the biological basis and clinical implications. *Progress in Neuro-Psychopharmacology and Biological Psychiatry*, 88, 401–417. <https://doi.org/10.1016/j.pnpb.2018.05.009>
- Di Martino, A., Yan, C. G., Li, Q., Denio, E., Castellanos, F. X., Alaerts, K., ... Milham, M. P. (2014). The autism brain imaging data exchange: Towards a large-scale evaluation of the intrinsic brain architecture in autism. *Molecular Psychiatry*, 19(6), 659–667. <https://doi.org/10.1038/mp.2013.78>
- Dichter, G. S., Felder, J. N., Green, S. R., Rittenberg, A. M., Sasson, N. J., & Bodfish, J. W. (2012). Reward circuitry function in autism spectrum disorders. *Social Cognitive and Affective Neuroscience*, 7(2), 160–172. <https://doi.org/10.1093/scan/nsq095>
- Du, J., Rolls, E. T., Cheng, W., Li, Y., Gong, W., Qiu, J., & Feng, J. (2019). Functional connectivity of the orbitofrontal cortex, anterior cingulate cortex, and inferior frontal gyrus in humans. *Cortex* in press.
- Frassle, S., Lomakina, E. I., Razi, A., Friston, K. J., Buhmann, J. M., & Stephan, K. E. (2017). Regression DCM for fMRI. *NeuroImage*, 155, 406–421. <https://doi.org/10.1016/j.neuroimage.2017.02.090>
- Freton, M., Lemogne, C., Bergouignan, L., Delaveau, P., Lehericy, S., & Fossati, P. (2014). The eye of the self: precuneus volume and visual perspective during autobiographical memory retrieval. *Brain Structure & Function*, 219(3), 959–968. <https://doi.org/10.1007/s00429-013-0546-2>
- Friston, K. (2009). Causal modelling and brain connectivity in functional magnetic resonance imaging. *PLoS Biology*, 7(2), e33. <https://doi.org/10.1371/journal.pbio.1000033>
- Friston, K. J., Kahan, J., Biswal, B., & Razi, A. (2014). A DCM for resting state fMRI. *NeuroImage*, 94, 396–407. <https://doi.org/10.1016/j.neuroimage.2013.12.009>
- Friston, K. J., Mechelli, A., Turner, R., & Price, C. J. (2000). Nonlinear responses in fMRI: The Balloon model, Volterra kernels, and other hemodynamics. *NeuroImage*, 12(4), 466–477. <https://doi.org/10.1006/nimg.2000.0630>
- Fuster, J. (2015). *The prefrontal cortex* (5th ed.). London: Academic Press.
- Gilson, M., Deco, G., Friston, K. J., Hagmann, P., Mantini, D., Betti, V., ... Corbetta, M. (2018). Effective connectivity inferred from fMRI transition dynamics during movie viewing points to a balanced reconfiguration of cortical interactions. *NeuroImage*, 180(Pt B), 534–546. <https://doi.org/10.1016/j.neuroimage.2017.09.061>
- Gilson, M., Moreno-Bote, R., Ponce-Alvarez, A., Ritter, P., & Deco, G. (2016). Estimation of directed effective connectivity from fMRI functional connectivity hints at asymmetries in the cortical connectome. *PLoS Computational Biology*, 12, e1004762.
- Goldman-Rakic, P. S. (1996). The prefrontal landscape: implications of functional architecture for understanding human mentation and the central executive. *Philosophical Transactions of the Royal Society B*, 351, 1445–1453.
- Gotts, S. J., Simmons, W. K., Milbury, L. A., Wallace, G. L., Cox, R. W., & Martin, A. (2012). Fractionation of social brain circuits in autism spectrum disorders. *Brain*, 135(Pt 9), 2711–2725. <https://doi.org/10.1093/brain/aww160>
- Hadjikhani, N., Joseph, R. M., Snyder, J., & Tager-Flusberg, H. (2007). Abnormal activation of the social brain during face perception in autism. *Human Brain Mapping*, 28(5), 441–449. <https://doi.org/10.1002/hbm.20283>

- Hasselmo, M. E., Rolls, E. T., & Baylis, G. C. (1989). The role of expression and identity in the face-selective responses of neurons in the temporal visual cortex of the monkey. *Behavioural Brain Research*, 32(3), 203–218.
- Hirshhorn, M., Grady, C., Rosenbaum, R. S., Winocur, G., & Moscovitch, M. (2012). The hippocampus is involved in mental navigation for a recently learned, but not a highly familiar environment: a longitudinal fMRI study. *Hippocampus*, 22(4), 842–852. <https://doi.org/10.1002/hipo.20944>
- Hull, J. V., Dokovna, L. B., Jacokes, Z. J., Torgerson, C. M., Irimia, A., & Van Horn, J. D. (2016). Resting-state functional connectivity in autism spectrum disorders: A review. *Frontiers in Psychiatry*, 7, 205. <https://doi.org/10.3389/fpsy.2016.00205>
- Kenet, T., Orekhova, E. V., Bharadwaj, H., Shetty, N. R., Israeli, E., Lee, A. K., ... Manoach, D. S. (2012). Disconnectivity of the cortical ocular motor control network in autism spectrum disorders. *NeuroImage*, 61(4), 1226–1234. <https://doi.org/10.1016/j.neuroimage.2012.03.010>
- Kesner, R. P., & Rolls, E. T. (2015). A computational theory of hippocampal function, and tests of the theory: New developments. *Neuroscience and Biobehavioral Reviews*, 48, 92–147. <https://doi.org/10.1016/j.neubiorev.2014.11.009>
- Kim, Y. S., Leventhal, B. L., Koh, Y. J., Fombonne, E., Laska, E., Lim, E. C., ... Grinker, R. R. (2011). Prevalence of autism spectrum disorders in a total population sample. *American Journal of Psychiatry*, 168(9), 904–912. <https://doi.org/10.1176/appi.ajp.2011.10101532>
- Koshino, H., Kana, R. K., Keller, T. A., Cherkassky, V. L., Minshew, N. J., & Just, M. A. (2008). fMRI investigation of working memory for faces in autism: Visual coding and underconnectivity with frontal areas. *Cerebral Cortex*, 18(2), 289–300. <https://doi.org/10.1093/cercor/bhm054>
- Lai, M. C., Lombardo, M. V., & Baron-Cohen, S. (2014). Autism. *Lancet*, 383(9920), 896–910. [https://doi.org/10.1016/S0140-6736\(13\)61539-1](https://doi.org/10.1016/S0140-6736(13)61539-1)
- Lavenex, P., & Amaral, D. G. (2000). Hippocampal-neocortical interaction: A hierarchy of associativity. *Hippocampus*, 10(4), 420–430. [https://doi.org/10.1002/1098-1063\(2000\)10:4<420::AID-HIPO8>3.0.CO;2-5](https://doi.org/10.1002/1098-1063(2000)10:4<420::AID-HIPO8>3.0.CO;2-5)
- Liptak, T. (1958). On the combination of independent tests. *Magyar Tudományos Akademia Matematikai Kutató Intézetének Közleményei*, 3, 171–197.
- Lombardo, M. V., Chakrabarti, B., Bullmore, E. T., Sadek, S. A., Pasco, G., Wheelwright, S. J., ... Baron-Cohen, S. (2010). Atypical neural self-representation in autism. *Brain*, 133(Pt 2), 611–624. <https://doi.org/10.1093/brain/awp306>
- Lundqvist, L.-O. (2015). Hyper-responsiveness to touch mediates social dysfunction in adults with autism spectrum disorders. *Research in Autism Spectrum Disorders*, 9, 13–20.
- Markov, N. T., Ercsey-Ravasz, M., Van Essen, D. C., Knoblauch, K., Toroczkai, Z., & Kennedy, H. (2013). Cortical high-density counterstream architectures. *Science*, 342(6158), 1238406. <https://doi.org/10.1126/science.1238406>
- Markov, N. T., Ercsey-Ravasz, M. M., Ribeiro Gomes, A. R., Lamy, C., Magrou, L., Vezoli, J., ... Kennedy, H. (2014). A weighted and directed interareal connectivity matrix for macaque cerebral cortex. *Cerebral Cortex*, 24(1), 17–36. <https://doi.org/10.1093/cercor/bhs270>
- Markov, N. T., & Kennedy, H. (2013). The importance of being hierarchical. *Current Opinion in Neurobiology*, 23(2), 187–194. <https://doi.org/10.1016/j.conb.2012.12.008>
- Markov, N. T., Vezoli, J., Chameau, P., Falchier, A., Quilodran, R., Huissoud, C., ... Kennedy, H. (2014). Anatomy of hierarchy: Feedforward and feedback pathways in macaque visual cortex. *Journal of Comparative Neurology*, 522(1), 225–259. <https://doi.org/10.1002/cne.23458>
- Marreiros, A. C., Kiebel, S. J., & Friston, K. J. (2008). Dynamic causal modelling for fMRI: A two-state model. *NeuroImage*, 39(1), 269–278. <https://doi.org/10.1016/j.neuroimage.2007.08.019>
- Maximo, J. O., Cadena, E. J., & Kana, R. K. (2014). The implications of brain connectivity in the neuropsychology of autism. *Neuropsychology Review*, 24(1), 16–31. <https://doi.org/10.1007/s11065-014-9250-0>
- Mitra, A., Snyder, A. Z., Tagliazucchi, E., Laufs, H., & Raichle, M. E. (2015). Propagated infra-slow intrinsic brain activity reorganizes across wake and slow wave sleep. *eLife*, 4, e10781. <https://doi.org/10.7554/eLife.10781>
- Padmanabhan, A., Lynch, C. J., Schaer, M., & Menon, V. (2017). The default mode network in autism. *Biological Psychiatry: Cognitive Neuroscience and Neuroimaging*, 2(6), 476–486. <https://doi.org/10.1016/j.bpsc.2017.04.004>
- Passingham, R. E. P., & Wise, S. P. (2012). *The neurobiology of the prefrontal cortex*. Oxford: Oxford University Press.
- Pierce, K., Haist, F., Sedaghat, F., & Courchesne, E. (2004). The brain response to personally familiar faces in autism: Findings of fusiform activity and beyond. *Brain*, 127(Pt 12), 2703–2716. <https://doi.org/10.1093/brain/awh289>
- Pierce, K., Muller, R. A., Ambrose, J., Allen, G., & Courchesne, E. (2001). Face processing occurs outside the fusiform 'face area' in autism: Evidence from functional MRI. *Brain*, 124(Pt 10), 2059–2073.
- Razi, A., Seghier, M. L., Zhou, Y., McColgan, P., Zeidman, P., Park, H. J., ... Friston, K. J. (2017). Large-scale DCMs for resting-state fMRI. *Network Neuroscience*, 1(3), 222–241. [https://doi.org/10.1162/NETN\\_a\\_00015](https://doi.org/10.1162/NETN_a_00015)
- Riquelme, I., Hatem, S. M., & Montoya, P. (2016). Abnormal pressure pain, touch sensitivity, proprioception, and manual dexterity in children with autism spectrum disorders. *Neural Plasticity*, 2016, 1723401. <https://doi.org/10.1155/2016/1723401>
- Rolls, E. T. (2014). *Emotion and decision-making explained*. Oxford: Oxford University Press.
- Rolls, E. T. (2016). *Cerebral cortex: Principles of operation*. Oxford: Oxford University Press.
- Rolls, E. T. (2018a). *The brain, emotion, and depression*. Oxford: Oxford University Press.
- Rolls, E. T. (2018b). The storage and recall of memories in the hippocampo-cortical system. *Cell and Tissue Research*, 373, 577–604. <https://doi.org/10.1007/s00441-017-2744-3>
- Rolls, E. T. (2019a). The cingulate cortex and limbic systems for emotion, action, and memory. *Brain Structure & Function*, 1–18. <https://doi.org/10.1007/s00429-019-01945-2>
- Rolls, E. T. (2019b). *The orbitofrontal cortex*. Oxford: Oxford University Press.
- Rolls, E. T. (2019c). The orbitofrontal cortex and emotion in health and disease, including depression. *Neuropsychologia*, 128, 14–43. <https://doi.org/10.1016/j.neuropsychologia.2017.09.021>

- Rolls, E. T., Cheng, W., Gilson, M., Gong, W., Deco, G., Lo, C. Z., ... Feng, J. (2019). Beyond the disconnectivity hypothesis of schizophrenia. *Cerebral Cortex*. <https://doi.org/10.1093/cercor/bhz1161>
- Rolls, E. T., Cheng, W., Gilson, M., Qiu, J., Hu, Z., Ruan, H., ... Feng, J. (2018). Effective connectivity in depression. *Biological Psychiatry: Cognitive Neuroscience and Neuroimaging*, 3(2), 187–197. <https://doi.org/10.1016/j.bpsc.2017.10.004>
- Rolls, E. T., & Deco, G. (2002). *Computational neuroscience of vision*. Oxford: Oxford University Press.
- Rolls, E. T., & Deco, G. (2010). *The noisy brain: Stochastic dynamics as a principle of brain function*. Oxford: Oxford University Press.
- Rolls, E. T., Joliot, M., & Tzourio-Mazoyer, N. (2015). Implementation of a new parcellation of the orbitofrontal cortex in the automated anatomical labeling atlas. *NeuroImage*, 122, 1–5. <https://doi.org/10.1016/j.neuroimage.2015.07.075>
- Rolls, E. T., Webb, T. J., & Deco, G. (2012). Communication before coherence. *European Journal of Neuroscience*, 36, 2689–2709.
- Rolls, E. T., & Wirth, S. (2018). Spatial representations in the primate hippocampus, and their functions in memory and navigation. *Progress in Neurobiology*, 171, 90–113. <https://doi.org/10.1016/j.pneurobio.2018.09.004>
- Scherf, K. S., Elbich, D., Minschew, N., & Behrmann, M. (2015). Individual differences in symptom severity and behavior predict neural activation during face processing in adolescents with autism. *NeuroImage: Clinical*, 7, 53–67. <https://doi.org/10.1016/j.nicl.2014.11.003>
- Treves, A., & Rolls, E. T. (1994). A computational analysis of the role of the hippocampus in memory. *Hippocampus*, 4, 374–391.
- Turova, T., & Rolls, E. T. (2019). Analysis of biased competition and cooperation for attention in the cerebral cortex. *Frontiers in Computational Neuroscience*, 13, 51. <https://doi.org/10.3389/fncom.2019.00051>
- Uddin, L. Q., Supekar, K., Lynch, C. J., Khouzam, A., Phillips, J., Feinstein, C., ... Menon, V. (2013). Salience network-based classification and prediction of symptom severity in children with autism. *JAMA Psychiatry*, 70, 869–879.
- Valdes-Sosa, P. A., Roebroeck, A., Daunizeau, J., & Friston, K. (2011). Effective connectivity: Influence, causality and biophysical modeling. *NeuroImage*, 58(2), 339–361. <https://doi.org/10.1016/j.neuroimage.2011.03.058>
- Van Hoesen, G. W. (1982). The parahippocampal gyrus. New observations regarding its cortical connections in the monkey. *Trends in Neuroscience*, 5, 345–350.
- Xia, M., Wang, J., & He, Y. (2013). BrainNet Viewer: A network visualization tool for human brain connectomics. *PLoS One*, 8(7), e68910.

## Supporting Information

Additional supporting information may be found online in the Supporting Information section at the end of the article.

**Appendix S1:** Supporting Information